

# Synthesis, Mesomorphism, and Unusual Magnetic Behaviour of Lanthanide Complexes with Perfluorinated Counterions

Yury G. Galyametdinov,<sup>\*,[a, b]</sup> Wolfgang Haase,<sup>[b]</sup> Larisa Malykhina,<sup>[a]</sup> Andrey Prosvirin,<sup>[a, b]</sup> Ildar Bikchantaev,<sup>[a, b]</sup> Ajdar Rakhmatullin,<sup>[a]</sup> and Koen Binnemans<sup>\*,[c]</sup>

**Abstract:** Lanthanide complexes of the Schiff base ligand 4-dodecyloxy-*N*-hexadecyl-2-hydroxybenzaldimine and with perfluorinated alkyl sulfate counterions were synthesised. All of the metal complexes show a smectic A mesophase. The viscosity of this mesophase is much lower than that of analogous compounds with nitrate or alkyl sulfate counterions. The behaviour of these new highly

anisotropic molecular magnetic materials was studied using high-temperature X-ray measurements in an external magnetic field and temperature-dependent magnetic susceptibility measure-

ments. The  $\mu_{\text{eff}}$ -versus-temperature curve is more comparable with those expected for nematic phases than for smectic phases. The luminescence spectrum of a Eu<sup>III</sup> compound shows that the values of the second rank crystal field parameters are very large. The huge magnetic anisotropy can be related to this strong crystal-field perturbation.

**Keywords:** lanthanides • liquid crystals • magnetic properties • metallomesogens

## Introduction

Research in the field of metal-based liquid crystals (metallomesogens) started about 25 years ago and the experience gained by different workers over this period now makes it possible to synthesise mesomorphic materials with desirable liquid-crystalline properties.<sup>[1]</sup> Several studies have been devoted to liquid-crystalline lanthanide complexes with salicylaldimine ligands.<sup>[2–11]</sup> These metallomesogens combine the interesting magnetic properties of the lanthanide with the advantages of supramolecular organisation in the mesophase. Lanthanide complexes can have a huge magnetic anisotropy

and magnetic birefringence,<sup>[3,5,10,16]</sup> or can be strongly luminescent.<sup>[17]</sup> Such substances could be appropriate building blocks for easily alignable soft magnetic molecular materials.<sup>[10]</sup> The molecules of a mesogenic compound in the liquid-crystalline phase can be aligned by applying an external magnetic field. For magnetic-field-induced alignment, the compounds need to have a nonzero magnetic anisotropy  $\Delta\chi$ . Moderate transition temperatures (less than 100 °C) are preferable to facilitate physical studies of these compounds in the mesophase. Low transition temperatures have been obtained by replacing nitrate or chlorine anions with alkyl sulfates. The transition temperatures of the alkyl sulfate complexes  $[\text{LnL}_3(\text{C}_n\text{H}_{2n+1}\text{SO}_4)_3]$  are 80 to 100 °C lower than the corresponding temperatures for chloride and nitrate derivatives.<sup>[6,8]</sup> A high magnetic anisotropy is not a sufficient condition for easy alignment of liquid crystals in an external magnetic field, and a mesophase with a low viscosity is also desirable. All of the metal complexes which have been prepared up to now (with nitrate, chloride, and alkyl sulfate counterions), displayed a very viscous mesophase.

We found that the viscosity of the mesophase could be reduced by replacing the alkyl sulfate counterions with the perfluorinated analogues  $\text{CF}_3(\text{CF}_2)_5\text{CH}_2\text{SO}_4^-$  or  $\text{CHF}_2(\text{CF}_2)_5\text{CH}_2\text{SO}_4^-$ . In the present study, we describe the synthesis, characterisation, magnetic, and luminescence properties of these lanthanide complexes of the Schiff base ligand 4-dodecyloxy-*N*-hexadecyl-2-hydroxybenzaldimine (Ligand L) with perfluorinated alkyl sulfate counterions. We also discuss how substitution of H atoms by F atoms has a strong influence on the mesomorphic and magnetic behaviour.

[a] Prof. Dr. Y. G. Galyametdinov, L. Malykhina, Dr. A. Prosvirin, Dr. I. Bikchantaev, Dr. A. Rakhmatullin  
Kazan Physical-Technical Institute  
Russian Academy of Sciences  
Sibirsky Tract 10/7, 420029 Kazan (Russia)  
Fax: (+7)84-32-76-50-75  
E-mail: Galyametdinov@sci.kcn.ru

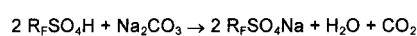
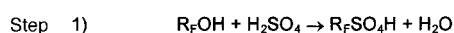
[b] Prof. Dr. Y. G. Galyametdinov, Prof. Dr. W. Haase, Dr. A. Prosvirin, Dr. I. Bikchantaev  
Institut für Physikalische Chemie  
Technische Universität Darmstadt  
Petersenstrasse 20, 64287 Darmstadt (Germany)

[c] Dr. K. Binnemans  
Katholieke Universiteit Leuven  
Department of Chemistry  
Celestijnenlaan 200F, 3001 Leuven (Belgium)  
Fax: (+32)16-32-79-92  
E-mail: koen.binnemans@chem.kuleuven.ac.be

Supporting information (the C,H,N analysis data of rare-earth complexes 1–20) for this article is available on the WWW under <http://www.wiley-vch.de/home/angewandte/> or from the author.

## Results and Discussion

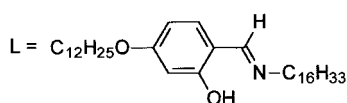
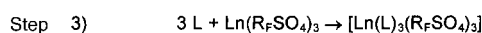
**Synthesis:** The lanthanide complexes were obtained in a three-step reaction, which is summarised in Scheme 1. In the first step, sodium perfluoroalkyl sulfates were prepared. In the second step two series of lanthanide perfluoroalkyl sulfates were synthesised by a metathesis reaction between a hydrated lanthanide chloride and sodium *1H,1H*-dodecafluoroheptyl sulfate (Series a) or *1H,1H,7H*-undecafluoroheptyl sulfate (Series b). Finally the lanthanide perfluoroalkyl sulfates reacted at room temperature with an equimolar amount of the corresponding Schiff base ligand (salicylaldimine, Ligand L). Ligand L was synthesised according to a literature procedure.<sup>[10]</sup> The lanthanide complexes precipitated as pale yellow powders. They were filtered, washed with ice-cold absolute ethanol, and dried in vacuo.



where  $R_F = \text{CF}_3(\text{CF}_2)_5\text{CH}_2$  (series a) or  $\text{CHF}_2(\text{CF}_2)_5\text{CH}_2$  (series b)



where  $\text{Ln}^{\text{III}} = \text{La}^{\text{III}}, \text{Ce}^{\text{III}}, \text{Pr}^{\text{III}}, \text{Nd}^{\text{III}}, \text{Sm}^{\text{III}}, \text{Eu}^{\text{III}}, \text{Gd}^{\text{III}}, \text{Tb}^{\text{III}}, \text{Dy}^{\text{III}}, \text{Ho}^{\text{III}}, \text{Er}^{\text{III}}, \text{Yb}^{\text{III}}$



Scheme 1. Synthesis of the lanthanide complexes with Schiff base ligands and perfluorinated alkyl sulfate counterions.

As shown in previous work,<sup>[9, 10]</sup> salicylaldimine ligands bind in a zwitterionic form to the central lanthanide ion. Based on C,H,N elemental analysis results, <sup>1</sup>H NMR data (at  $\delta = 12.79$ , an NH signal was observed with an integrated intensity corresponding to three protons), and magnetic moment measurements at room temperature, it was found that the stoichiometry of the complexes is consistent with the formula  $[\text{Ln}(\text{L})_3(\text{R}_F\text{SO}_4)_3]$ , in which  $R_F$  stands for  $\text{CF}_3(\text{CF}_2)_5\text{CH}_2$  (Series a) or  $\text{CHF}_2(\text{CF}_2)_5\text{CH}_2$  (Series b).

**Liquid crystalline behaviour:** Ligand L is not mesomorphic,<sup>[10]</sup> but all of the complexes show liquid crystallinity. The thermal behaviour of the lanthanide complexes has been investigated by hot stage polarising microscopy, by differential scanning calorimetry (DSC), and by high temperature X-ray diffraction. Under the microscope both series of complexes exhibit a fan-shaped texture, which is typical for the smectic A mesophase ( $S_A$ ). It is noteworthy that the substances obtained in the present work exhibit a more fluid mesophase than previously described lanthanide-containing metallomesogens. This reduction in viscosity is obtained by using counterions with perfluorinated alkyl chains. In Table 1 the phase

Table 1. Mesophase behaviour of the lanthanide complexes with perfluorinated counterions  $[\text{Ln}(\text{L})_3(\text{R}_F\text{SO}_4)_3]$ .

No.	Ln	$R_F$ <sup>[a]</sup>	Cr- $S_A$ <sup>[b, c]</sup> $T$ [°C]	$S_A$ -I <sup>[b]</sup> $T$ [°C]	$\Delta T$ [°C] <sup>[d]</sup>
1	La	a	110	121	11
2	Pr	a	113	120	7
3	Nd	a	114	122	8
4	Eu	a	110	125	15
5	Gd	a	106	119	13
6	Tb	a	103	119	16
7	Ho	a	96	120	24
8	Er	a	98	125	27
9	La	b	111	131	20
10	Ce	b	114	131	17
11	Pr	b	115	135	20
12	Nd	b	109	133	24
13	Sm	b	106	131	25
14	Eu	b	106	132	26
15	Gd	b	108	126	18
16	Tb	b	99	128	29
17	Dy	b	102	125	23
18	Ho	b	98	125	27
19	Er	b	98	140	42
20	Yb	b	103	138	35

[a]  $R_F = \text{CF}(\text{CF}_2)_5\text{CH}_2$  (Series a);  $R_F = \text{CHF}_2(\text{CF}_2)_5\text{CH}_2$  (Series b). [b] Cr = crystalline solid,  $S_A$  = smectic A phase, I = isotropic liquid. [c] Because of the often complex thermal behaviour of the compounds in the solid state, we ignore here the presence of a possible highly ordered mesophase ( $S_X$ ) between the crystalline state and the  $S_A$  phase. [d]  $\Delta T$  = mesophase stability range of the  $S_A$  phase (in °C).

transition temperatures of the complexes are presented. The transition temperature dependence on the type of lanthanide ion is presented in Figure 1 and Figure 2. In Series a, the width of the mesophase stability range increases over the lanthanide series. This behaviour is opposite to what was found for Schiff

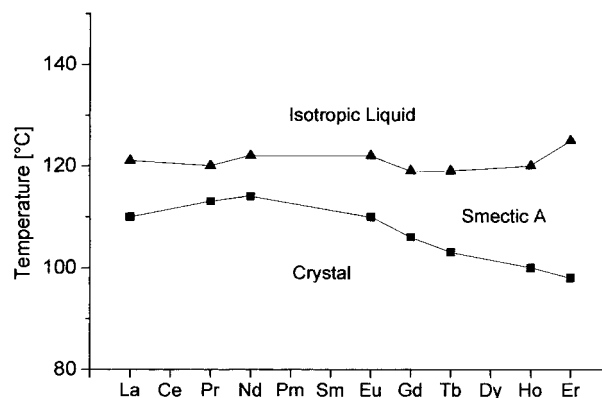


Figure 1. Dependence of the transition temperature of the  $[\text{LnL}_3(\text{R}_F\text{SO}_4)_3]$  complexes on the type of lanthanide ion (for Series a,  $R_F = \text{CF}_3(\text{CF}_2)_5\text{CH}_2$ ): ■: crystal  $\rightarrow$   $S_A$  transition; ▲:  $S_A \rightarrow$  isotropic liquid transition.

base complexes with nitrate counterions.<sup>[7]</sup> The same behaviour is found for Series b. Remarkable for this type of compounds is that the clearing points of Er<sup>III</sup> complex **19** and Yb<sup>III</sup> complex **20** are distinctively higher than those of the other lanthanide complexes.

Because the perfluorinated alkyl sulfate counterions have a much larger molar volume than nitrate or chloride ions, the

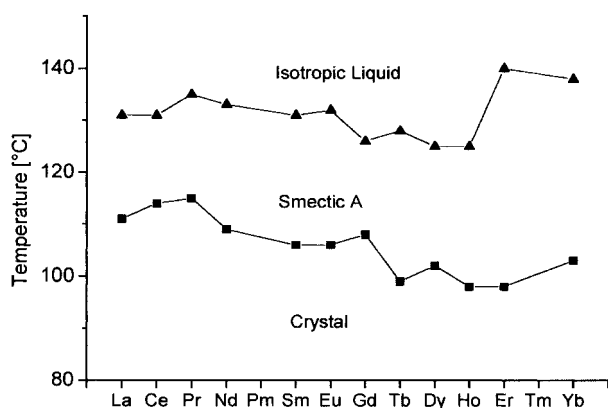


Figure 2. Dependence of the transition temperature of the  $[\text{LnL}_3(\text{R}_F\text{SO}_4)_3]$  complexes on the type of lanthanide ion (for Series b,  $\text{R}_F = \text{CHF}_2(\text{CF}_2)_5\text{CH}_2$ ): ■: crystal  $\rightarrow$   $\text{S}_A$  transition; ▲:  $\text{S}_A \rightarrow$  isotropic liquid transition.

former counterions have a greater influence on molecular packing in the crystal than nitrates or chlorides do. This larger molecular volume reduces the interlayer interaction energy in the crystal and as a consequence the melting points decrease. The smaller interlayer interactions result in a less viscous mesophase (observable as enhanced fluidity of the samples in the microscope). One of the characteristics of these metal-mesogens is their ability to form glassy mesophases, so that the structure of the mesophase can be frozen into the solid state. Additionally, we observed some degree of supercooling for the clearing points, that is the clearing points were at a higher temperature when the compounds were heated than when the compounds were cooled.

The liquid-crystalline structure of the lanthanide complexes was also characterised by X-ray diffraction at elevated temperatures. As an example, the X-ray diffraction patterns of the erbium complex  $[\text{ErL}_3[\text{CHF}_2(\text{CF}_2)_5\text{CH}_2\text{SO}_4]_3]$  (**8**) at the different temperatures are shown in Figure 3. Two sharp reflections in the small-angle region ( $2\theta = 2.64^\circ$  and  $5.60^\circ$ ) and a diffuse reflection around  $2\theta = 19^\circ$  were detected. This X-ray pattern indicates the presence of a disordered smectic phase. There are some features (sharpness of the peaks) that indicate that highly ordered and crystal (recrystallisation process) phases are present. The thickness of the smectic layer  $d$  obtained by application of Bragg's law to the small-angle peak is  $44.5 \text{ \AA}$ . The lengths of the Schiff base, Ligand L, and of the complex were calculated by molecular modelling to be  $43.4 \text{ \AA}$  and  $47.0 \text{ \AA}$ , respectively. The differences between the calculated and experimental data can be explained by penetration of the alkyl chains of one layer into another. Alternatively the smaller experimental smectic layer distances can be explained by strong thermal motion of the alkyl chains on heating in mesophase.

The DSC plot of  $\text{Gd}^{\text{III}}$  compound **5** is shown in Figure 4. In DSC traces we could observe an endothermic peak before the melting point (determined by optical microscopy) for several samples. Although the sample does not become fluid at this transition point, microscopic investigation showed that the compound behaves like a wax in this case. From X-ray data it was not possible to unambiguously assign this phase. Although further investigation is necessary, we can already

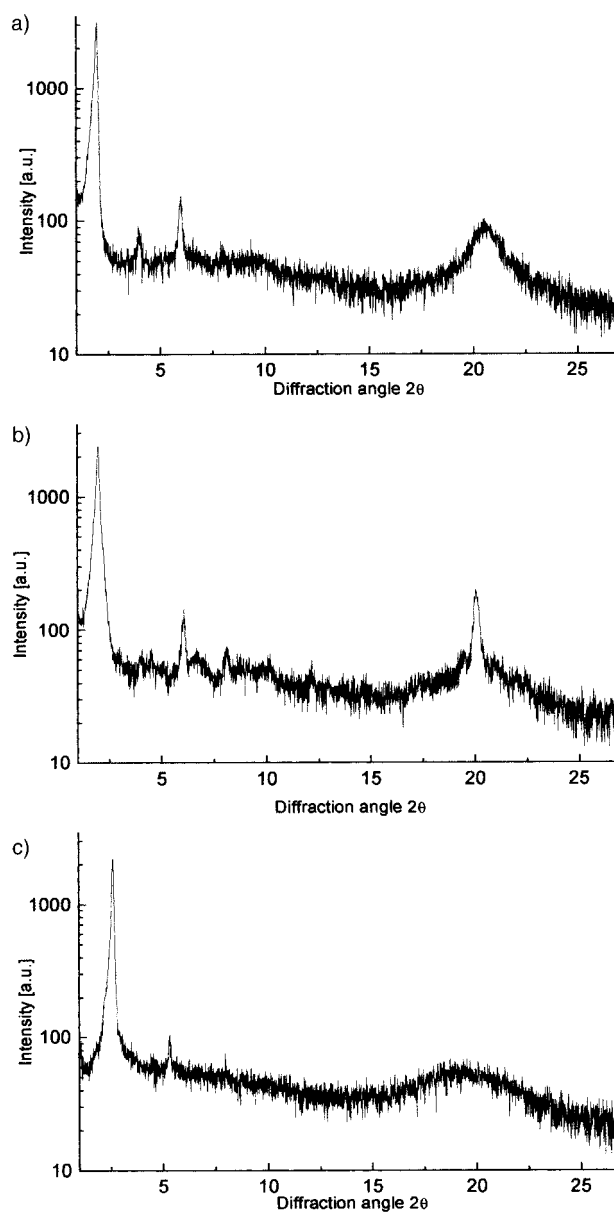


Figure 3. X-ray diffraction patterns of  $\text{Er}^{\text{III}}$  complex **19** at the different temperatures: a) starting material,  $T = 25^\circ\text{C}$ ,  $d = 45 \text{ \AA}$ ; b)  $\text{S}_x$  phase,  $T = 90^\circ\text{C}$ ,  $d = 44 \text{ \AA}$ ; c)  $\text{S}_A$  phase,  $T = 115^\circ\text{C}$ ,  $d = 34 \text{ \AA}$ .

anticipate the existence of a highly ordered smectic mesophase ( $\text{S}_x$ ). Most likely, this phase corresponds to a state with partially molten alkyl chains. As will be discussed further, an  $\text{S}_A \rightarrow \text{S}_x$  mesophase could also be observed by magnetic measurements.

#### Orientalional behaviour of mesophase in a magnetic field:

The behaviour of the new compounds in an external magnetic field was investigated by means of X-ray diffraction and by magnetic susceptibility measurements. With X-ray diffraction measurements on an oriented mesophase in a magnetic field, it is possible to determine the alignment direction of the molecules in the magnetic field and to determine the sign of the magnetic anisotropy  $\Delta\chi$ . If the molecular long axis is parallel to the direction of the magnetic field, the magnetic anisotropy  $\Delta\chi$  is positive, whereas a perpendicular alignment

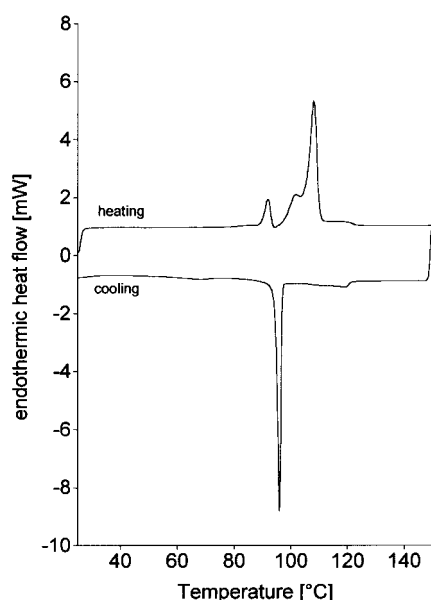


Figure 4. DSC trace of Gd<sup>III</sup> compound **5** (first heating–cooling run). Endothermic peaks point upwards. The complex melting behaviour is clearly visible.

corresponds to a negative sign of  $\Delta\chi$ . Temperature-dependent magnetic susceptibility measurements and the sign of  $\Delta\chi$  are necessary to determine the magnitude of the magnetic anisotropy  $\Delta\chi$ . In the X-ray diffraction experiments, the capillary containing the sample was heated to a temperature several degrees above the clearing point and slowly cooled down in a permanent magnetic field of 1.2 T until the mesophase was reached. The sample was exposed to X-rays for several hours. The photoplates of the oriented samples showed two sharp inner reflections and a diffuse reflection in the wide-angle area, which gives evidence for a liquid-crystalline S<sub>A</sub> phase. For the Eu<sup>III</sup> and Er<sup>III</sup> complexes **14** and **19** we observed a sharp peak at 45 Å, corresponding to the interlayer distance in a direction parallel to the magnetic field. The average value of the angle between the director and the molecular long axis is equal to 20° (on a photoplate  $\phi$  corresponds to the width of the first reflex). We can calculate the order parameter according to formula  $S = (3\cos^2\phi - 1)/2$ . For the oriented mesophase,  $S \approx 0.8$  for the rigid part of the molecule. In a direction perpendicular to the magnetic field we observed two peaks: a diffuse reflection at 11 Å (corresponding to the distance between the rigid parts of the compounds), while a diffuse reflection (4.2 Å) is provided by the intralayer distance between the molten aliphatic chains. The width of the first reflection ( $\approx 20^\circ$ ) corresponds to the order parameter  $S \approx 0.8$  for the rigid part of the molecule as in the former case. The width of the second reflection is  $\approx 45^\circ$ , which corresponds to the order parameter  $S \approx 0.2$  for the molten alkyl chains of the molecule.

We also obtained the photoplates of the X-ray diffractograms for compounds [TbL<sub>3</sub>{CHF<sub>2</sub>(CF<sub>2</sub>)<sub>5</sub>CH<sub>2</sub>SO<sub>4</sub>}<sub>3</sub>] (**16**) and [HoL<sub>3</sub>{CF<sub>3</sub>(CF<sub>2</sub>)<sub>5</sub>CH<sub>2</sub>SO<sub>4</sub>}<sub>3</sub>] (**7**) aligned by a magnetic field in the S<sub>A</sub> phase. The photoplates for Tb<sup>III</sup> and Ho<sup>III</sup> compounds **16** and **7** look the same as those of the former compounds but rotated by 90°; a sharp peak at 45 Å in a direction

perpendicular to the magnetic field and two diffuse peaks in a direction parallel to the magnetic field were observed. We can thus conclude that the complexes of Er<sup>III</sup> and Eu<sup>III</sup> are oriented with their molecular long axis parallel to the magnetic field, while the Tb<sup>III</sup> and Ho<sup>III</sup> complexes are oriented with their long molecular axis perpendicular to the magnetic field. This behaviour is in agreement with what can be expected on the basis of knowledge of the sign of the magnetic anisotropy for the different lanthanide ions.<sup>[18]</sup>

**Magnetic susceptibility measurements:** To investigate the orientation behaviour of the mesogenic lanthanide derivatives in a magnetic field and to obtain quantitative information about the value of the magnetic anisotropy, we carried out temperature-dependent magnetic susceptibility measurements in the liquid-crystalline phase. The substances were initially heated to the isotropic phase and then cooled slowly to the smectic phase in an applied magnetic field of 1.5 T. An increase of the magnetic susceptibility and thus of the effective magnetic moment  $\mu_{\text{eff}}$  was observed at the isotropic-to-mesophase transition (Figure 5). This effect can be

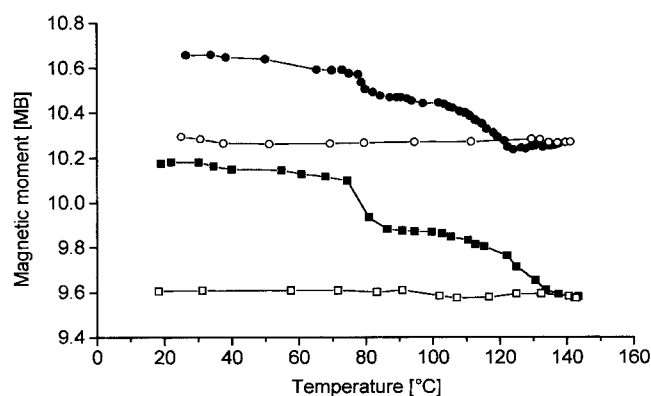


Figure 5. Effective magnetic moments  $\mu_{\text{eff}}$  (MB) versus temperature  $T$  [°C] of Ho<sup>III</sup> complex **18** and Er<sup>III</sup> complex **19** in an applied magnetic field of 1.5 T: ○: heating run for **18**; ●: cooling run for **18**; □: heating run for **19**; ■: cooling run for **19**.

explained as a magnetic-field-induced alignment in the liquid-crystalline phase of a magnetically anisotropic sample with its axis of maximum susceptibility  $\chi_{\text{or}}$  parallel to the magnetic field. In the isotropic phase, one obtains the isotropic susceptibility ( $\chi_{\text{iso}}$ ), whereas in the oriented mesophase, the maximum component of the  $\chi$ -tensor ( $\chi_{\text{or}}$ ) is recorded. The alignment of the mesophase is only observed when cooling from the isotropic phase and not when heating the solid compound. The lower viscosity of the mesophase close to the clearing point makes alignment easier than for a mesophase close to the melting point. If  $\Delta\chi = \chi_{\parallel} - \chi_{\perp} < 0$ , the molecular long axis is oriented perpendicular to the direction of the magnetic field and in the oriented phase  $\chi_{\perp}$  will be measured. Therefore we can calculate the magnitude of  $\Delta\chi$  including orientation behaviour, from X-ray measurement of the negative sign of  $\Delta\chi = \chi_{\parallel} - \chi_{\perp}$  using  $\Delta\chi = -3(\chi_{\text{or}} - \chi_{\text{iso}})$  for the Ho<sup>III</sup> and Tb<sup>III</sup> compounds. In the Eu<sup>III</sup>, La<sup>III</sup>, Gd<sup>III</sup> and Er<sup>III</sup> compounds we can propose a positive sign and  $\Delta\chi = 1.5(\chi_{\text{or}} - \chi_{\text{iso}})$ . The values  $(\chi_{\text{or}} - \chi_{\text{iso}})$  were calculated in the

following manner:  $(\chi_{\text{or}} - \chi_{\text{iso}}) \approx [\mu_{\text{eff}}^2(\text{Cr}) - \mu_{\text{eff}}^2(\text{I})]/(8T_{\text{S-Cr}})$ . The experimental  $\chi_{\text{or}} - \chi_{\text{iso}}$  data at the phase transition temperature and the estimated values of the magnetic anisotropy  $\Delta\chi$  for  $\text{LnL}_3\text{X}_3$  compounds are given in Table 2.

In contrast to previous results<sup>[4, 10]</sup> in which we observed one steep jump, for the present series we have two jumps in the magnetic susceptibility value during the cooling process. This could indicate the existence of an additional (more ordered) mesophase between the crystalline and  $S_A$  phases.<sup>[19]</sup> This is in agreement with the X-ray diffraction and DSC data. In the case of compounds with a high magnetic anisotropy, temperature-dependent magnetic susceptibility measurements are a sensitive method for detecting phase transitions. In the literature, not many examples are known of the use of magnetic susceptibility measurements for observing phase transitions. For instance, Bahadur reported a jump in the magnetic susceptibility curve of *N*-(*p*-hexyloxybenzylidene)-*p*-toluidine at the nematic to smectic B transition.<sup>[20]</sup> The increase in the effective magnetic moment  $\mu_{\text{eff}}$  at the clearing point is not as sharp as was observed for the complexes with nitrate counterions. The magnetic moment smoothly increases when cooling the smectic mesophase, in a way similar to the nematic mesophase.<sup>[21]</sup> The unusual shape of the  $\mu_{\text{eff}}$ -versus-temperature curve will be the subject of further theoretical study.

Interestingly, the magnetic anisotropy values of the investigated compounds are very sensitive to the nature of the counterion structure. For example,  $\Delta\chi$  for the  $\text{Ho}^{\text{III}}$  derivatives **7** and **18** (Table 2) changes from  $-9100 \times 10^6 \text{ cm}^3 \text{ mol}^{-1}$ , to  $-12830 \times 10^6 \text{ cm}^3 \text{ mol}^{-1}$  when the counterion is changed from  $\text{CF}_3(\text{CF}_2)_5\text{CH}_2\text{SO}_4$  to  $\text{CHF}_2(\text{CF}_2)_5\text{CH}_2\text{SO}_4$ . The highest values of  $\Delta\chi$  are found for  $\text{Dy}^{\text{III}}$  and  $\text{Ho}^{\text{III}}$  complexes with orientation of the molecular long axis perpendicular to the direction of the applied magnetic field. In our previous work the maximum value of the magnetic anisotropy was found for the  $\text{Tb}^{\text{III}}$  complexes.<sup>[4, 10]</sup> This can be explained by the difference in the order parameter, because the observed value of the magnetic anisotropy of the samples is proportional to  $\Delta\chi$  multiplied by the order parameter of the liquid crystal *S*. The difference in viscosity of the present and former series can account for the difference in orientation behaviour. Another reason could be a change in the structure of the first coordination sphere and thus to a change in the crystal-field parameters. The crystal-field parameters have a significant influence on the magnetic anisotropy. We compared the

magnetic susceptibility anisotropies of the fluorine-containing Schiff base complexes of the lanthanides with the values obtained for the previously described<sup>[4, 10]</sup> derivatives with nitrate and sulfate counterions (Table 3). It is evident from the

Table 3. Dependence of the magnetic susceptibility anisotropy ( $\Delta\chi$ ) on the type of counterion in lanthanide complexes  $\text{LnL}_3\text{X}_3$  with Schiff base ligands.

Ln	X	L		$\Delta\chi^{[a]}$
		<i>n</i>	<i>m</i>	
Ho	NO <sub>3</sub>	12	16	-4756
Ho	CHF <sub>2</sub> (CF <sub>2</sub> ) <sub>5</sub> CH <sub>2</sub> SO <sub>4</sub>	12	16	-12840
Dy	NO <sub>3</sub>	14	18	-7794
Dy	C <sub>12</sub> H <sub>25</sub> SO <sub>4</sub>	14	18	-9804
Dy	CHF <sub>2</sub> (CF <sub>2</sub> ) <sub>5</sub> CH <sub>2</sub> SO <sub>4</sub>	12	16	-19470
Tb	NO <sub>3</sub>	14	18	-4665
Tb	CHF <sub>2</sub> (CF <sub>2</sub> ) <sub>5</sub> CH <sub>2</sub> SO <sub>4</sub>	12	16	-8220
Tb	C <sub>8</sub> H <sub>17</sub> SO <sub>4</sub>	12	16	-3910

[a] All susceptibilities  $\chi$  are expressed in the units  $10^6 \text{ cm}^3 \text{ mol}^{-1}$  at the temperature  $T_{\text{c-s}}$ .

data in Table 3 that the fluorinated derivatives of the different ions always have the highest magnetic anisotropy. The fluorinated complexes of  $\text{Dy}^{\text{III}}$  exhibit the highest values of  $\Delta\chi$  in the series of different metals and counterions. Because the mesophase of the lanthanide complexes can be supercooled to a glassy mesophase, it is possible to obtain anisotropic magnetic materials by cooling the mesophase in a magnetic field.

**Luminescence properties:** Because the magnitude of magnetic anisotropy  $\Delta\chi$  depends on the strength of the crystal-field perturbation,<sup>[22]</sup> we measured the luminescence spectrum of  $\text{Eu}^{\text{III}}$  compound **14** to have an estimate of the crystal-field strength (Figure 6). When the compound was irradiated with light of 393 nm (ca.  $25445 \text{ cm}^{-1}$ ) a red photoluminescence could be observed. It is noteworthy that the luminescence intensity is much stronger than that of corresponding compounds with nitrate counterions. All of the transitions start from the  $^5\text{D}_0$  excited state and the luminescence peaks correspond to  $^5\text{D}_0 \rightarrow ^7\text{F}_j$  transitions. The luminescence spec-

Table 2. Magnetic properties of the compounds  $[\text{Ln}(\text{L})_3(\text{R}_f\text{SO}_4)_3]$ .

Compound	Ln	$R_f^{[a]}$	$T$ [°C]	$\mu_{\text{eff}}$ [BM]				Orientation to H	$(\chi_{\text{or}} - \chi_{\text{iso}})^{[b]}$	$\Delta\chi^{[b]}$	
				Cr- $S_A$	$S_A$ -I	theor	I				$S_A$
<b>6</b>	Tb	a	80	109	9.7	9.29	9.57	9.63	⊥	2280	-6840
<b>7</b>	Ho	a	80	120	10.5	10.24	10.47	10.65	⊥	3035	-9100
<b>12</b>	Nd	b	104	121	3.6	3.62	3.69	3.70	⊥	195	-580
<b>14</b>	Eu	b	98	124	3.4	3.79	3.97	3.97		470	700
<b>16</b>	Tb	b	79	108	9.7	9.44	9.69	9.84	⊥	2740	-8220
<b>17</b>	Dy	b	93	102	10.5	10.10	10.67	11.00	⊥	6490	-19470
<b>18</b>	Ho	b	81	122	10.5	9.97	10.30	10.56	⊥	4280	-12840
<b>19</b>	Er	b	80	130	9.5	9.58	9.88	10.15		3985	5980

[a]  $R_f = \text{CF}(\text{CF}_2)_5\text{CH}_2$  (Series a);  $R_f = \text{CHF}_2(\text{CF}_2)_5\text{CH}_2$  (Series b). [b] All susceptibilities  $\chi$  are listed in units  $10^6 \text{ cm}^3 \text{ mol}^{-1}$  at the temperature  $T_{\text{S-Cr}}$ .

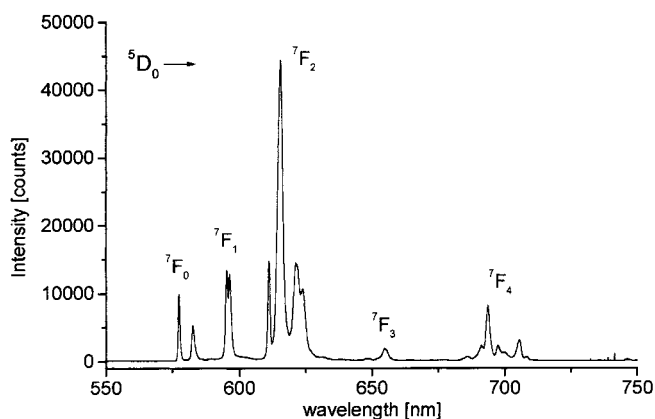


Figure 6. Luminescence spectrum of  $\text{Eu}^{\text{III}}$  compound **14** at 77 K. The excitation wavelength was 393 nm.

trum is well resolved at 77 K and crystal-field fine structure could be observed. The  $^5\text{D}_0 \rightarrow ^7\text{F}_0$  transition could be detected at  $17320\text{ cm}^{-1}$  (577.36 nm). Other peaks were observed in this spectral region at  $17164\text{ cm}^{-1}$  (582.61 nm),  $16798\text{ cm}^{-1}$  (595.30 nm), and  $16768\text{ cm}^{-1}$  (596.39 nm). Although the peaks at 16798 and  $16768\text{ cm}^{-1}$  could easily be assigned to the  $^5\text{D}_0 \rightarrow ^7\text{F}_1$  transition, assignment of the peak at  $17164\text{ cm}^{-1}$  was more difficult. This peak could in principle be assigned to the  $^5\text{D}_0 \rightarrow ^7\text{F}_1$  transition or to the  $^5\text{D}_0 \rightarrow ^7\text{F}_0$  transition (in the case that two nonequivalent sites are present in the compound). However, there is strong evidence that this transition belongs to the  $^5\text{D}_0 \rightarrow ^7\text{F}_1$  transition group. In this case, the crystal-field levels of the  $^7\text{F}_1$  manifold are located at 156, 522, and  $552\text{ cm}^{-1}$ , so that the barycenter is at  $410\text{ cm}^{-1}$ . According to Antic-Fidancev, a correlation exists between the position of the  $^5\text{D}_0$  level of  $\text{Eu}^{3+}$  and the position of the barycenter of the  $^7\text{F}_1$  manifold.<sup>[23]</sup> If the  $^5\text{D}_0$  level is at  $17300\text{ cm}^{-1}$ , the barycenter of the  $^7\text{F}_1$  manifold is expected at about  $400\text{ cm}^{-1}$ , which is in good agreement with our experimental values ( $17320$  and  $410\text{ cm}^{-1}$ , respectively). Because especially second rank ( $k=2$ )  $B^k_q$  crystal-field parameters contribute to the magnetic anisotropy, we determined the  $B^2_0$  and  $B^2_2$  crystal-field parameters using the analytical expression for the matrix elements given by G rller-Walrand and Binnemans.<sup>[24]</sup> Not enough experimental data are available for determination of all crystal-field parameters. Although the actual crystal-field symmetry is  $C_1$ , we took  $C_{2v}$  symmetry as an approximation in order to avoid complex crystal-field parameters. We use the Wybourne normalisation (with  $C^k_q$  operators).<sup>[25]</sup> We found the following values for the second rank crystal-field parameters:  $|B^2_0| = 1170\text{ cm}^{-1}$  and  $|B^2_2| = 56\text{ cm}^{-1}$  for the case that the crystal-field level at  $156\text{ cm}^{-1}$  is the  $\langle 0|$  state. The value of the crystal-field parameter  $B^2_0$  is very large, and only a few compounds are known with a larger second-rank crystal field effect.<sup>[26]</sup> Because the crystal-field parameters do not drastically change over the lanthanide series, we can assume that the other lanthanide ions also have a large  $B^2_0$  crystal-field parameter. Therefore we can find evidence for the origin of the huge magnetic anisotropy of our compound in the strong crystal-field effect.

## Conclusion

New liquid-crystalline lanthanide complexes with perfluorinated alkyl sulfate counterions and having low transition temperatures and a highly fluid mesophase have been synthesised. Two jumps in the magnetic susceptibility curve on the alignment of the materials in a mesophase in a magnetic field were detected. Both X-ray and magnetic data give evidence for the existence of a highly ordered mesophase. The magnetic behaviour of the lanthanide metallomesogens is rather sensitive to the type of counterion. The behaviour of smectic mesogenic compounds in a magnetic field (a smooth increase of the magnetic anisotropy with decrease in temperature) is similar to that observed for nematic liquid crystals. In fact, new highly anisotropic molecular materials have been obtained by magnetic field alignment of mesogenic complexes of the lanthanides with perfluorinated alkyl sulfate counterions. The huge magnetic anisotropy can be related to a strong crystal-field perturbation.

## Experimental Section

**General:** NMR spectra were recorded on a UNITY-300 spectrometer (299.95 MHz,  $^1\text{H}$ ; 282.23 MHz,  $^{19}\text{F}$ ) equipped with a 5 mm probe. The chemical shifts of  $^1\text{H}$  were measured relative to internal  $\text{CHCl}_3$  ( $\delta = 7.26$ ). The chemical shifts of  $^{19}\text{F}$  were measured relative to external  $\text{C}_6\text{F}_6$  ( $\delta = -163$ ). Temperatures and textures of phase transitions were determined by a polarisation microscope equipped with a hot stage and with a computer-driven temperature controller giving an accuracy better than  $\pm 0.05^\circ\text{C}$ . Differential scanning calorimetry (DSC) measurements were carried out on a Mettler-Toledo DSC 821e module (scan rate of  $10^\circ\text{Cmin}^{-1}$  under a nitrogen flow). The high temperature X-ray measurements were obtained with a STOE STADI 2 diffractometer, with a linear position sensitive detector (STOE mini PSD). Monochromatic  $\text{CuK}\alpha$  radiation was obtained using a curved germanium detector (111 plane). The sample was placed in a Lindemann glass capillary and heated in an electric furnace. The temperature of the furnace was controlled by a Eurotherm temperature controller. The X-ray diffractogram of the mesophase oriented by a magnetic field was recorded on a flat film. The sample was in a Lindemann capillary and was aligned by two permanent magnets of 1.2 T. The temperature-dependent magnetic susceptibilities were recorded on a Faraday type magnetometer, using a home-built heating device.<sup>[27]</sup> The measurements presented were done using a computer-controlled Cahn RG microbalance and a Bruker B-MN 200/40 power supply.<sup>[28]</sup> The applied field was 1.5 T. In order to achieve good alignment of the molecules, cooling rates were  $1^\circ\text{Cmin}^{-1}$  or less. The molar susceptibilities were corrected for the underlying diamagnetism applying Pascal's scheme.<sup>[29]</sup> Magnetic moments were obtained using the formula  $\mu_{\text{eff}}/\mu_{\text{B}} = 2.828(\chi\text{T})^{1/2}$ . Luminescence spectra were recorded at ambient temperature and at liquid nitrogen temperature (77 K) using a home-built apparatus. A water-cooled 450 W xenon lamp was used as the excitation source. Wavelength selection was achieved by a Sciencetech Model 9050 monochromator. Luminescence light was measured at an angle of  $90^\circ$  with respect to the excitation beam. The emission light was analysed using a McPherson monochromator ( $1200\text{ linesmm}^{-1}$ ). For detection, the signal of a photomultiplier was measured using a photon counting system (Stanford Research Systems SR400 Two Channel Gated Photon Counter). Wavelength calibration achieved by using the emission lines of a mercury lamp. The samples were cooled in a bath cryostat (Oxford Instruments). For the luminescence spectra, the metal complexes were mixed with KBr and pressed to a pellet.

**Sodium 1*H,1H*-dodecafluoroheptyl sulfate ( $\text{CF}_3(\text{CF}_2)_5\text{CH}_2\text{OSO}_3\text{Na}$ ):** 1*H,1H*-Dodecafluoroheptanol-1 (2 mL, 50 mmol) was added dropwise to oleum (2 mL, 40 mmol) with cooling ( $0^\circ\text{C}$ ) and stirring. The reaction mixture was stirred for 30 min, and the temperature was allowed to rise to room temperature. The mixture was poured into ice-cold water (50 mL)

and was neutralised to pH 7 with powdered sodium carbonate. The product was precipitated by adding sodium chloride. The white powder was filtered off and recrystallised from ethanol (2.2 g, 85%). Elemental analysis calcd (%) for  $C_7H_5F_{13}O_4Sn$  (452.12): C 18.60, H 0.45, F 54.63; found: C 18.85, H 0.47, F 54.85.

**Lanthanum tris[1H, 1H-dodecafluoroheptyl sulfate ( $La[CF_2(CF_2)_5CH_2O-SO_3]_3$ ):** Ethanolic solutions of lanthanum chloride heptahydrate (0.028 g, 0.1 mmol) and sodium 1H,1H-dodecafluoroheptyl sulfate (0.15 g, 0.3 mmol) were mixed at room temperature. The sodium chloride precipitate was filtered off. The product was precipitated from the filtrate by partially evaporating the solvent, yielding 0.12 g (71%) of a white powder. Elemental analysis calcd (%) for  $C_{21}H_6F_{39}O_{12}S_3La$  (1425.75): C 17.68, H 0.42, F 51.95; found: C 17.80, H 0.50, F 51.99.

**Lanthanum complex 1:** Lanthanum tris[1H,1H-dodecafluoroheptyl sulfate] (0.069 g, 0.01 mmol) was added to an ethanol solution of Ligand L (0.08 g, 0.03 mmol) at 30 °C. The precipitate was filtered off and dried in vacuo, yielding 0.09 g (85%) of a yellow powder.  $^1H$  NMR (300 MHz,  $CDCl_3$ ):  $\delta$  = 0.90 (t, 3H;  $CH_3$ ), 1.20–1.50 (m, 47H;  $CH_2$ ,  $CH_3$ ), 1.71 (m, 2H;  $NCH_2CH_2$ ), 2.24 (m, 2H;  $OCH_2CH_2$ ), 3.57 (t, 2H;  $NCH_2$ ), 3.82 (t, 2H;  $OCH_2$ ), 4.02 (m, 2H;  $SOCH_2$ ), 6.25 (d,  $J$  = 8.1 Hz, 1H; H-aryl), 6.64 (d, 1H; H-aryl), 6.99 (d,  $J$  = 8.1 Hz, 1H; H-aryl), 7.79 (s, 1H;  $CH=N$ ), 12.79 (s, 1H; NH);  $^{19}F$  NMR (282.23 MHz,  $CDCl_3$ ):  $\delta$  = -123.23 (m, 2F), -125.43 (s, 2F), -126.51 (s, 2F), -126.83 (s, 2F), -132.94 (s, 2F), -140.30 (d, 3F); elemental analysis calcd (%) for  $C_{126}H_{195}F_{39}N_3O_{18}S_3La$  (3015.9): C 50.18, H 6.51, N 1.39; found: C 50.21, H 6.48, N 1.44.

**All other complexes:** were prepared as above on a similar scale. The C,H,N analysis results are available as Supporting Information.

## Acknowledgements

Yu. G. Galyametdinov, W. Haase, I. Bikhantaev, and A. Prosvirin thank the Deutsche Forschungsgemeinschaft (grant 436RUS/113/401) and Volkswagen Stiftung (grant I/72818). Yu. Galyametdinov and K. Binnemans are indebted to the NATO for financial support (Collaborative Linkage Grant PST.CLG.974907). K. Binnemans is a Postdoctoral Fellow of the Fund for Scientific Research Flanders (Belgium) and thanks Prof. C. Görrler-Walrand for providing laboratory facilities. Financial support by the K.U. Leuven (GOA 98/03) and by the F.W.O.-Flanders (G.0243.99) is gratefully acknowledged. Luminescence spectra were recorded by R. Van Deun, the crystal-field parameters were determined by K. Driesen and the C,H,N analyses done by P. Bloemen.

- [1] a) A. M. Giroud-Godquin and P. M. Maitlis, *Angew. Chem.* **1991**, *103*, 370; *Angew. Chem. Int. Ed. Engl.* **1991**, *30*, 375; b) P. Espinet, M. A. Esteruelas, L. A. Oro, J. L. Serrano, E. Sola, *Coord. Chem. Rev.* **1992**, *117*, 215; c) S. A. Hudson, P. M. Maitlis, *Chem. Rev.* **1993**, *93*, 861; d) D. W. Bruce, *J. Chem. Soc., Dalton Trans.* **1993**, 2983; e) A. P. Polishchuk, T. V. Timofeeva, *Russ. Chem. Rev.* **1993**, *62*, 291; f) *Metal-lobesogens, Synthesis, Properties and Applications* (Ed.: J. L. Serrano), VCH, Weinheim, **1996**; g) D. W. Bruce in *Inorganic Materials*, 2nd ed (Eds.: D. W. Bruce, D. O'Hare), Wiley, Chichester, **1996**, Chapter 8, p. 429; h) A. M. Giroud-Godquin, *Coord. Chem. Rev.* **1998**, *178–180*, 1485; i) B. Donnio, D. W. Bruce, *Struct. Bonding* **1999**, *95*, 193; j) S. R. Collinson, D. W. Bruce in *Transition Metals in Supramolecular Chemistry* (Ed.: J. P. Sauvage), Wiley, New York, **1999**, Chapter 7, p. 285.
- [2] Yu. G. Galyametdinov, G. I. Ivanova, I. V. Ovchinnikov, *Bull. Acad. Sci. USSR, Div. Chem. Sci. (Engl. Transl.)* **1991**, *40*, 1109.
- [3] Yu. G. Galyametdinov, G. I. Ivanova, A. V. Prosvirin, O. Kadkin, *Russ. Chem. Bull.* **1994**, *43*, 938.
- [4] Yu. G. Galyametdinov, M. A. Athanassopoulou, K. Griesar, O. Kharitonova, E. A. Soto Bustamante, L. Tinchurina, I. Ovchinnikov, W. Haase, *Chem. Mater.* **1996**, *8*, 9222.
- [5] Yu. G. Galyametdinov, G. Ivanova, I. Ovchinnikov, A. Prosvirin, D. Guillon, B. Heinrich, D. A. Dunmur, D. W. Bruce, *Liq. Cryst.* **1996**, *20*, 831.
- [6] K. Binnemans, Yu. G. Galyametdinov, S. R. Collinson, D. W. Bruce, *J. Mater. Chem.* **1998**, *8*, 1551.
- [7] K. Binnemans, R. Van Deun, D. W. Bruce, Yu. G. Galyametdinov, *Chem. Phys. Lett.* **1999**, *300*, 6470.
- [8] Yu. G. Galyametdinov, G. I. Ivanova, I. V. Ovchinnikov, K. Binnemans, D. W. Bruce, *Russ. Chem. Bull.* **1999**, *48*, 385.
- [9] K. Binnemans, D. W. Bruce, S. R. Collinson, R. Van Deun, Yu. G. Galyametdinov, F. Martin, *Phil. Trans. Royal Soc.* **1999**, *A 357*, 3063.
- [10] K. Binnemans, Yu. G. Galyametdinov, R. Van Deun, D. W. Bruce, S. R. Collinson, A. P. Polishchuk, I. Bikhantaev, W. Haase, A. V. Prosvirin, L. Tinchurina, I. Litvinov, A. Gubajdullin, A. Rakhmatullin, K. Uytterhoeven, L. Van Meervelt, *J. Am. Chem. Soc.* **2000**, *122*, 4335.
- [11] F. Martin, S. R. Collinson, D. W. Bruce, *Liq. Cryst.* **2000**, *27*, 859.
- [12] Yu. G. Galyametdinov, M. Athanassopoulou, W. Haase, I. V. Ovchinnikov, *Russ. J. Coord. Chem.* **1995**, *21*, 718.
- [13] M. Gerloch, D. J. Mackey, *J. Chem. Soc. Dalton Trans.* **1972**, 415, and references therein.
- [14] M. L. Kahn, M. Verelst, P. Lecante, C. Mathonniere, O. Kahn, *Eur. J. Inorg. Chem.* **1999**, 527.
- [15] R. S. Prosser, V. B. Volkov, I. V. Shiyonovskaya, *Biophys. J.* **1998**, *75*, 2163.
- [16] S. G. Vul'fson, *Molecular magnetochemistry*, Gordon and Breach, Amsterdam, **1998**, p. 350, and references therein.
- [17] a) J. C. G. Bünzli, *Luminescent Probes*, in *Lanthanide Probes in Life, Chemical and Earth Sciences, Theory and Practice* (Eds.: J. C. G. Bünzli, G. R. Choppin), Elsevier, Amsterdam, **1989**, Chapter 7, p. 219; b) G. Blasse, B. C. Grabmaier, *Luminescent Materials*, Springer, Berlin, **1994**.
- [18] B. Bleaney, *J. Magn. Res.* **1972**, *8*, 91.
- [19] F. Hardouin, M. F. Achard, G. Sigaud, H. Gasparoux, *Mol. Cryst. Liq. Cryst.* **1977**, *39*, 241.
- [20] B. Bahadur, *J. Chem. Phys.* **1977**, *67*, 3272.
- [21] I. H. Ibrahim, W. Haase, *J. Phys. (France)* **1979**, *40*, C3,164.
- [22] A. T. Casey, S. Mitra, "Magnetic Behaviour of Lanthanide Compounds", in *Theory and Applications of Molecular Paramagnetism* (Eds.: E. A. Boudreaux, L. N. Mulay), Wiley, New York, **1976**, Chapter 5, pp. 271–316.
- [23] E. Antic-Fidancev, *J. Alloys Compds.* **2000**, *300*, 2.
- [24] C. Görrler-Walrand, K. Binnemans in *Handbook on the Physics and Chemistry of Rare Earths* (Eds.: K. A. Gschneidner, Jr., L. Eyring), Vol. 23, North-Holland Publishers, Amsterdam, **1996**, Chapter 155, pp. 121–283.
- [25] B. G. Wybourne, *Spectroscopic Properties of Rare Earths*, Interscience, New York, **1965**.
- [26] K. Binnemans and C. Görrler-Walrand, *Chem. Phys. Lett.* **1995**, *245*, 75.
- [27] L. Merz and W. Haase, *J. Chem. Soc. Dalton Trans.* **1980**, 875.
- [28] S. Gehring, P. Fleischhauer, H. Paulus, W. Haase, *Inorg. Chem.* **1993**, *32*, 54.
- [29] A. Weiss, H. Witte, *Magnetochemie*, Verlag Chemie, Weinheim, **1973**, p. 345.

Received: June 16, 2000 [F2544]